electronics

MDPI

Article

Distributed Adaptive Fault-Tolerant Control for Leaderless/Leader–Follower Multi-Agent Systems against Actuator and Sensor Faults

Zhengyu Ye, Yuehua Cheng, Ziquan Yu and Bin Jiang *

College of Automation Engineering, Nanjing University of Aeronautics and Astronautics, Nanjing 210016, China; kasoll076@nuaa.edu.cn (Z.Y.); chengyuehua@nuaa.edu.cn (Y.C.); yuziquan@nuaa.edu.cn (Z.Y.)
* Correspondence: binjiang@nuaa.edu.cn

Abstract: The faults of actuators and sensors can lead to abnormal operations or even system faults in multi-agent systems (MASs). To address this issue, this paper proposes an adaptive fault-tolerant control (FTC) algorithm for leaderless/leader–follower MASs against actuator and sensor faults. First, extended states integrating the fault components are constructed and the MAS is transformed into a descriptor system form. Then, a sliding-mode observer is designed for the transformed MAS. Based on the estimated MAS states and faults, adaptive FTC algorithms are developed, which update the control gains with the distributed tracking error. Finally, numerical simulations demonstrate that the proposed method can guarantee MAS stability against actuator and sensor faults.

Keywords: adaptive control; fault tolerant control; multi-agent systems; sensor fault; sliding mode

Citation: Ye, Z.; Cheng, Y.; Yu, Z.; Jiang, B. Distributed Adaptive Fault-Tolerant Control for Leaderless/Leader–Follower Multi-Agent Systems against Actuator and Sensor Faults. *Electronics* **2023**, *12*, 2924. https://doi.org/10.3390/electronics12132924

Academic Editor: Fernando De la Prieta Pintado

Received: 29 May 2023
Revised: 30 June 2023
Accepted: 30 June 2023
Published: 3 July 2023

1. Introduction

Multi-agent systems (MASs) have many virtues in comparison with the conventional control systems such as greater robustness, flexibility, and adaptability, which empower the MAS with the capability to deal with more complex task scenarios [1,2]. As a result of these advantages, MAS has been widely applied in fields such as drones formation, multi-robots coordination, and supply chain management [3–12]. The outstanding advantages of MASs and their extensive engineering applications make them an important direction for modern control and robotics technology development, which will have profound impacts on various fields in the future. However, the scalability and complexity of MAS make it difficult for conventional centralized control methods to meet the requirements. The theoretical value and application prospects make MASs attract a lot of research attention.

Currently, the main research directions for control methods in MASs include distributed control theory, flocking algorithms, adaptive control, and intelligent control, etc. [13–15]. Among them, the research results of distributed control are the richest. According to the structure of MASs, distributed control can be divided into two categories: leaderless and leader–follower. The control objective of leaderless MAS is to achieve consensus of MAS [16], whereas the control objective of leader–follower MAS is to track the leader's state [17]. According to whether the communications are unidirectional or bidirectional, MASs can also be divided into two categories: directed graphs and undirected graphs, which makes the leader–follower become a special case in directed graphs [18]. In [19], adaptive discontinuous control protocols are studied to achieve fixed-time consensus of nonlinear MASs in leader-following and leaderless cases. A consensus-based formation control strategy of discrete MASs is investigated in [20], where bounded uncertain time-delays and directed switching topologies are considered. A consensus control scheme with time-varying coupling weights is investigated for linear MASs subjected to heterogeneous Brownian disturbances and directed topologies in [21], where the distributed controller is designed by utilizing Riccati inequalities and the coupling weights are updated

according to consensus error. Overall, as a popular research direction, distributed control has attracted much research efforts from many researchers, and the existing research results are abundant. However, many research results only focus on the design of control methods and consider relatively ideal scenarios: assuming that the precise system state is known and no faults occurred in the system, making the methods studied more theoretically valuable but weakening their engineering feasibility.

In practical applications, MASs contain a large number of agents distributed in space, and each agent has to face different environmental challenges, this places the MASs at risk of sensor and actuator faults. The component faults will cause the controller to be unable to accurately perceive the measurement of the system state or correctly execute control instructions, resulting in a degradation in the control performance of the MAS [22–27]. The fault of a single agent can affect the normal operation of neighboring agents through distributed control protocols, causing individual faults to escalate into a wider range of faults that threaten the stability of the MAS. However, due to the large scale and wide distribution of MASs, maintenance difficulties and long repair cycles of their sensors and actuators undermine the availability of the system. To facilitate real-world implementation, distributed control requires more comprehensive problem formulations and solutions embedding fault diagnosis and FTC modules. Specifically, in fault-afflicted scenarios where part of the system information is unavailable or unreliable, distributed reasoning and estimation methods should collaborate to recover the missing information causing by insufficient measurement or sensor faults. Robust and adaptive control paradigms should be investigated to handle uncertainties and maintain system stability when faults occur. On the whole, fault diagnosis (FD) and fault-tolerant control (FTC) of these two types of faults are urgent issues to address in the design of MASs.

At present, there are numerous research achievements on FD and FTC methods for MASs. In [28], a consensus tracking control scheme is designed to handle abrupt and incipient faults for MAS under fixed and switching topologies. An adaptive FTC is investigated for MAS where the parameter is updated online based on the local state information in [29]. In [30], an FTC algorithm for time-varying formation control is presented for MAS to ensure stability against the impact of actuator faults, specifically efficiency loss, and bias. A distributed adaptive fault-tolerant containment controller is designed to address actuator bias faults in MASs featuring multiple leaders by introducing observer-based techniques in [31]. In [32], a decentralized output sliding-mode FTC scheme with adaptive laws is proposed for heterogeneous MASs subjected to matched/unmatched disturbances and actuator faults. A resilient distributed observer-based FTC scheme is studied for MASs subjected to actuator faults and denial-of-service attacks in [33]. However, the studies mentioned above have primarily examined actuator faults and neglected the possibility of sensor faults. Diagnosing and handling sensor faults typically involves techniques such as filtering, estimating, or fault detection and isolation, which aim to mitigate the impact of inaccurate sensor readings on the control system's output. A method of diagnosing distributed sensor faults with $L_2 - L_\infty$ performance is explored in [34]. An algorithm for fault-tolerant output regulation is proposed for leader–follower MASs in the presence of sensor faults in [35], which guarantees convergence of all output tracking errors. Furthermore, a distributed FTC algorithm based on sliding mode and radial basis function neural networks is studied in [36].

Compared with actuator faults, the design of FD and FTC methods for sensor faults faces greater challenges, because sensor faults destroy the observation of the system state, making it impossible to accurately obtain state feedback [37,38]. This makes the design of observers and controllers extremely tricky. Effectively addressing sensor fault problems is key to improving system stability, safety, and reliability. Some scholars believe that sensor faults are not very valuable for research, because with the progress of production and technology, the accuracy and reliability of sensors have been greatly improved, and the miniaturization of sensors also makes hardware redundancy of sensors feasible. However, for MASs, the scale effect makes sensor redundancy an expensive solution. Moreover,

the design of MASs often involves miniaturized agents, and hardware redundancy can cause an increase in agent volume, thus making the MAS cumbersome. To put it another way, even for conventional single-machine systems, sensor redundancy can increase power consumption and require the design of filtering algorithms for data fusion. Additionally, for many systems, sensor redundancy can encroach upon the system's payload capacity, making it a limited means of preventing sensor faults, such as in the case of miniaturized unmanned aerial vehicles and spacecraft. Therefore, the importance of designing FD and FTC methods for sensor faults is just as important as doing so for actuator faults.

Indeed, distributed control is a frontier hot research topic, which has attracted broad attention and extensive research from the control community. The literature contains profuse theoretical results on distributed consensus protocols and cooperative control strategies that address system observability and controllability under ideal assumptions. Nevertheless, many results overlook system uncertainties and faults that are commonly encountered in real applications, compromising practical applicability. While rich theoretical results have been obtained, distributed control still awaits substantial development to enhance its implementation capability in practical systems. A promising direction is to integrate distributed control with fault diagnosis, fault tolerance, and adaptation. This can lead to a holistic solution that addresses challenges from both theoretical and practical perspectives, making distributed control fully ready for real-world deployment in critical infrastructures and applications.

Addressing the issues of actuator and sensor faults in leaderless/leader–follower MASs, this paper proposes a distributed adaptive FTC method based on sliding mode observers. The main contributions are:

1. The descriptor system approach is introduced to handle actuator and sensor faults in MASs. By extending the system state, the system transformation turns the component faults into the uncertainty of the transformed system, and the system is transformed into a descriptor system form so that fault diagnosis and state estimation can be achieved simultaneously.
2. A sliding mode observer is designed for the transformed descriptor dynamics to take advantage of the insensitivity of unknown input observers to uncertainty. By utilizing the sliding mode technique, the uncertainty of the transformed system is suppressed such that the estimation errors converge and the extended states are estimated.
3. Based on the obtained estimation of system state and faults, a distributed adaptive fault-tolerant control protocol is designed. The control gains are updated based on the distributed tracking error so that the MAS can maintain stability in the presence of actuator and sensor faults.

The rest of this paper is organized as follows: Section 2 provides the theoretical preliminaries and problem formulation. Section 3 is divided into three parts, where Part 1 conducts a descriptor system transformation and designs an observer based on sliding mode, while Parts 2 and 3, respectively, focus on the design of FTC methods for leaderless and leader–follower MASs. Section 4 presents numerical simulations, and Section 5 concludes the paper.

Notations: For the sake of brevity in subsequent expressions, certain symbol definitions are introduced herein. Let $1_l = [1, 1, \ldots, 1]^\top \in \mathbb{R}^l$, $0_{l_1 \times l_2}$ be a l_1-by-l_2 zero matrix, and $I_l \mathbb{R}^{l \times l}$ be an identity matrix. For a vector v, denote $\|v\| = \sqrt{v^\top v}$ as the norm function, and $\text{sign}(v) = \frac{v}{\|v\|}$ as the signum function, especially $\text{sign}(0) = 0$. For a matrix M, M^+ and $M^\top$ are the pseudo inverse and transpose, respectively, and $M^{-\top} = (M^{-1})^\top$. The Kronecker product is represented by $\otimes$. $\text{diag}(*)$ and $\text{blkdiag}(*)$ are the diagonal and block diagonal functions, respectively.

2. Preliminaries and Problem Formulation

2.1. Preliminaries

Graph Theory

The communication connections of MAS are described with an undirected graph $\mathcal{G} = (v, \varepsilon, \mathcal{A})$, where $v = \{v_1, \ldots, v_N\}$ is the agents set, $\varepsilon \subseteq v \times v$ is the connections set where $\varepsilon_{ij} \in \varepsilon$ represents the connection from agent i to agent j, and $\mathcal{A} = [a_{ij}] \in \mathbb{R}^{N \times N}$ is the adjacency matrix. For $\mathcal{A}$, $a_{ij} > 0$ if $\varepsilon_{ij} \in \varepsilon$, $a_{ij} = 0$ if $\varepsilon_{ij} \notin \varepsilon$ or $i = j$. Let $\mathcal{D} = \text{diag}(d_1, d_2, \ldots, d_N)$ in which $d_i = \sum_{i=1}^{N} a_{ij}$, then the Laplacian matrix can be calculated by $\mathcal{L} = \mathcal{D} - \mathcal{A}$. Similarly, the connections from agents to leader are denoted with $\mathcal{B} = \text{diag}(b_1, \ldots, b_N)$, where $b_i = 1$ if agent i can access the leader's information, otherwise $b_i = 0$.

2.2. Problem Formulation

Consider the MAS consists of N agents with linear dynamics. The dynamics of the i-th agent are formulated as follows. The dynamics of the i-th agent $(i = 1, \ldots, N)$ is formulated as

$$\begin{cases} \dot{x}_i = Ax_i + Bu_i + F_a f_{ai} \\ y_i = Cx_i + F_s f_{si} \end{cases}, \tag{1}$$

where $x_i \in \mathbb{R}^{n_x}$, $y_i \in \mathbb{R}^{n_y}$, $u_i \in \mathbb{R}^{n_u}$, $f_{ai} \in \mathbb{R}^{n_a}$, and $f_{si} \in \mathbb{R}^{n_s}$ are the system states, measurement output, control input, actuator fault, and sensor fault, respectively. $A \in \mathbb{R}^{n_x \times n_x}$, $B \in \mathbb{R}^{n_x \times n_u}$, $C \in \mathbb{R}^{n_y \times n_x}$, $F_a \in \mathbb{R}^{n_x \times n_a}$, and $F_s \in \mathbb{R}^{n_y \times n_s}$ are the system matrices.

The subsequent theoretical derivation is conducted on the basis of the following assumptions:

Assumption 1. *The graph that describes the communications among the MAS is connected.*

Assumption 2. *The actuators fault f_{ai} and sensor fault f_{si} are bounded and satisfy the conditions for all $i = 1, \ldots, N$: $\|f_{ai}\| \leq r_a$, $\|\dot{f}_{ai}\| \leq r_{ad}$, and $\|f_{si}\| \leq r_s$, where r_a, r_{ad}, and r_s are known positive constants.*

Assumption 3. *The dimensionality of faults in actuators and sensors satisfies the condition of $n_a + n_s \leq n_y$. Furthermore, the parameter matrices F_a and F_s are column full-rank matrices.*

Assumption 4. *The matrix rank of B and F_a satisfies the condition of* $\text{rank}([B, F_a]) = \text{rank}(B)$.

Remark 1. *The effectiveness of fault diagnosis depends on reliable system measurement. If the faults fully compromise measurement credibility, FD becomes impossible. Assumption 3 constrains the sensor fault dimensionality such that measurements retain partial observability and faults remain inferable.*

Remark 2. *From the perspective of mathematics, Assumption 4 implies that the column space of matrix F_a is a subspace of the column space of matrix B. From an engineering perspective, actuator faults only occur on actuator components. Therefore, the number of actuators determines the number of actuator faults, and the deployment of actuators determines how the actuator faults affect system dynamics. A common way to deal with it is to set $F_a = B$, but we consider the case where $F_a \neq B$ to conserve the generality of the model. Assumption 4 implies that the number of actuator faults is always less than or equal to the number of actuator outputs, and any deviation caused by actuator faults can be compensated for.*

Remark 3. *Actuator faults can typically be modeled in additive form and multiplicative form, i.e., $u_i^* = (1 - \rho_i)u_i + \varpi_i$, where u_i^* is the faulty actuator output, ρ_i symbolizes the coefficient of efficiency degradation, and ϖ_i is the bias fault. This equation can be converted into additive form $u_i^* = u_i + (\varpi_i - \rho_i u_i)$. Furthermore, by denoting $\varpi_i^* \triangleq (\varpi_i - \rho_i u_i)$ and combining with the cases in which $F_a \neq B$, the form of Equation (1) can be obtained.*

This paper aims to develop FTC for MAS (1) ensuring stability despite actuator and sensor faults. For leaderless MASs, the control objective is consensus, i.e., $\lim_{t\to\infty} x_i - \frac{1}{N}\sum_{j=1}^{N} x_j = 0$. For leader–follower MASs, the objective is tracking the leader's state x_0, i.e., $\lim_{t\to\infty} x_i - x_0 = 0$.

3. Main Results

Constructing an extended state $\bar{x}_i \triangleq \left[x_i^\top, f_{ai}^\top, f_{si}^\top\right]^\top$, the original system dynamics (1) can be transformed in the following descriptor form.

$$\begin{cases} \bar{E}\dot{\bar{x}}_i = \bar{A}\bar{x}_i + \bar{B}u_i + \bar{F}\bar{f}_i \\ y_i = \bar{C}\bar{x}_i \end{cases}, \tag{2}$$

where $\bar{f}_i \triangleq \left[(\dot{f}_{ai} + f_{ai})^\top, f_{si}^\top\right]^\top$ is the augmented uncertainty, $\bar{E} \triangleq \text{blkdiag}(I_{n_x+n_a}, 0_{n_s\times n_s})$, $\bar{C} \triangleq \left[C, 0_{n_y\times n_a}, F_s\right]$, and other matrices are given as

$$\bar{A} \triangleq \begin{bmatrix} A & F_a & \\ & -I_{n_a} & \\ & & -I_{n_s} \end{bmatrix}, \bar{B} \triangleq \begin{bmatrix} B \\ 0_{n_a\times n_u} \\ 0_{n_s\times n_u} \end{bmatrix}, \bar{F} \triangleq \begin{bmatrix} 0_{n_x\times n_a} & \\ I_{n_a} & 0_{n_a\times n_s} \\ & I_{n_s} \end{bmatrix}.$$

Note that in the descriptor system (2), the sensor faults f_{si} are incorporated into the augmented state $\bar{x}_i$, leading to the output y_i being solely dependent on $\bar{x}_i$. Hence, designing an observer for the descriptor system (2) is concerned only with attenuating the effects of the uncertainty term $\bar{f}_i$. Moreover, adopting the descriptor approach incorporates actuator fault f_{ai} and f_{si} into the extended state $\bar{x}_i$. Any stable observer for (2) can then simultaneously estimate x_i, f_{ai} and f_{si}.

3.1. Sliding Mode Observer

Note that $\bar{E}$ is singular as (2) is descriptor, with unknown input $\bar{f}_i$. Therefore, unknown input observer (UIO) is a suitable approach since it is insensitive to unknown input signals.

A sliding mode-based UIO is designed for the i-th agent $(i = 1, \ldots, N)$ by defining an intermediate variable $\hat{z}_i$:

$$\begin{cases} \bar{S}\dot{\hat{z}}_i = (\bar{A} - L_p\bar{C})\hat{z}_i + \bar{B}u_i + L_s v_{si} + \bar{K}y_i \\ \hat{\bar{x}}_i = \hat{z}_i + \bar{S}^{-1}L_D y_i \end{cases}, \tag{3}$$

where $\bar{n} \triangleq n_x + n_a + n_s$, v_{si} is the sliding mode term, $\bar{S} \in \mathbb{R}^{\bar{n}\times\bar{n}}$ is a non-singular matrix, $L_p \in \mathbb{R}^{\bar{n}\times n_y}$, $\bar{K} \in \mathbb{R}^{\bar{n}\times n_y}$ and $L_D \in \mathbb{R}^{\bar{n}\times n_y}$ are gain matrices designed later.

Lemma 1. *There exists a matrix L_D such that: (a) $\bar{S} \triangleq \bar{E} + L_D\bar{C}$ is non-singular; (b) $\bar{C}\bar{S}^{-1}L_D = I_{n_s}$; (c) $\bar{A}\bar{S}^{-1}L_D = -\bar{N}$.*

Proof. By recalling $\text{rank}(F_s) = n_s$ from Assumption 3, it follows that

$$\text{rank}\begin{bmatrix}\bar{E}\\ \bar{C}\end{bmatrix} = \text{rank}\begin{bmatrix} I_{n_x} & & \\ & I_{n_a} & \\ C & 0_{n_y\times n_a} & F_s \end{bmatrix} = \bar{n}. \tag{4}$$

Let L_D be defined by

$$L_D \triangleq \begin{bmatrix} 0_{(n_x+n_a)\times n_y} \\ \gamma M \end{bmatrix}, \tag{5}$$

where $\gamma > 0$, and $M \triangleq (F_s^\top F_s)^{-1}F_s^\top$.

Based on the fact that $\text{rank}(F_s) = n_s < n_y$, one has $MF_s = I_{n_s}$. Subsequently, $\bar{S}$ and $\bar{S}^{-1}$ can be obtained as follows

$$\bar{S} = \bar{E} + L_D\bar{C} = \begin{bmatrix} I_{n_x} & & \\ & I_{n_a} & \\ \gamma M\bar{C} & 0_{n_s\times n_a} & \gamma I_{n_s} \end{bmatrix}, \bar{S}^{-1} = \begin{bmatrix} I_{n_x} & & \\ & I_{n_a} & \\ -M\bar{C} & 0_{n_s\times n_a} & \frac{1}{\gamma} I_{n_s} \end{bmatrix}. \tag{6}$$

Furthermore, it can be derived that

$$\bar{C}\bar{S}^{-1}L_D = I_{n_s}, \bar{A}\bar{S}^{-1}L_D = -\begin{bmatrix} 0_{n_x\times n_y} \\ 0_{n_a\times n_y} \\ M \end{bmatrix}. \tag{7}$$

Let $N \triangleq \left[0^\top_{n_x\times n_y}, 0^\top_{n_a\times n_y}, M^\top\right]^\top$. The proof ends. □

Adding $L_D\bar{C}\dot{\bar{x}}_i$ to both sides of (2) derives

$$\bar{S}\dot{\bar{x}}_i = \bar{E}\dot{\bar{x}}_i + L_D\bar{C}\dot{\bar{x}}_i = \bar{A}\bar{x}_i + \bar{B}u_i + \bar{F}\bar{f}_i + L_D\bar{C}\dot{\bar{x}}_i. \tag{8}$$

It follows from (3) that

$$\begin{aligned} \bar{S}\dot{\hat{\bar{x}}}_i =& \bar{S}\left[\dot{\hat{z}}_i + \bar{S}^{-1}L_D\dot{y}_i\right] \\ =& (\bar{A} - L_p\bar{C})\hat{z}_i + \bar{B}u_i + L_s v_{si} + \bar{K}y_i + L_D y_i \\ =& (\bar{A} - L_p\bar{C})\hat{\bar{x}}_i - (\bar{A} - L_p\bar{C})\bar{S}^{-1}L_D y_i + \bar{B}u_i + \bar{K}y_i + L_s v_{si} + L_D\bar{C}\dot{\bar{x}}_i. \end{aligned} \tag{9}$$

Define the estimation error as $\tilde{\bar{x}}_i \triangleq \hat{\bar{x}}_i - \bar{x}_i$. Let $\bar{K}$ be determined by $\bar{K} \triangleq (\bar{A} - L_p\bar{C})\bar{S}^{-1}L_D + L_p$. Subtracting (8) from (9) and multiplying both sides by $\bar{S}^{-1}$, the following results can be obtained.

$$\dot{\tilde{\bar{x}}}_i = \bar{S}^{-1}\left[(\bar{A} - L_p\bar{C})\tilde{\bar{x}}_i - \bar{F}\bar{f}_i + L_s v_{si}\right]. \tag{10}$$

Let the matrix L_s be determined by $L_s \triangleq \bar{F}$, and a switching surface s_i be design as $s_i \triangleq H\bar{C}\tilde{\bar{x}}_i$, where $H \in \mathbb{R}^{(n_a+n_s)\times n_y}$ is a matrix determined such that $(P_2\bar{S}^{-1}\bar{F})^\top = H\bar{C}$ holds.

The sliding mode-based feedback term v_{si} is designed as

$$v_{si} = -(r_a + r_{ad} + r_s + \epsilon)\text{sign}(s_i) \tag{11}$$

where ϵ is a positive constant.

Lemma 2. *There exists a matrix L_p such that the following LMI holds:*

$$P\bar{S}^{-1}(\bar{A} - L_p\bar{C}) + (\bar{A} - L_p\bar{C})^\top\bar{S}^{-\top}P \preceq -Q, \tag{12}$$

where $\varrho > 0$, and $P \in \mathbb{R}^{\bar{n}\times\bar{n}}$ and $Q \in \mathbb{R}^{\bar{n}\times\bar{n}}$ are symmetric positive definite matrices.

Proof. There must be a positive definite matrix $R \in \mathbb{R}^{\bar{n}\times\bar{n}}$ such that the following inequality holds for matrix $\bar{S}^{-1}\bar{A}$:

$$\text{Re}\left[\lambda_i(-R - \bar{S}^{-1}\bar{A})\right] < 0, (i = 1, \ldots, \bar{n}) \tag{13}$$

Therefore, there exists a positive definite matrix P such that

$$-(R + \bar{S}^{-1}\bar{A})^\top P - P(R + \bar{S}^{-1}\bar{A}) = -\bar{C}^\top\bar{C}. \tag{14}$$

Let L_p be determined by $L_p \triangleq P^{-1}\bar{S}\bar{C}$, the following result can be obtained.

$$\left[R+\bar{S}^{-1}(\bar{A}-L_p\bar{C})\right]^{\top}P+P\left[R+\bar{S}^{-1}(\bar{A}-L_p\bar{C})\right]=-\bar{C}^{\top}\bar{C}. \tag{15}$$

Furthermore, it can be derived that

$$\left[\bar{S}^{-1}(\bar{A}-L_p\bar{C})\right]^{\top}P+P\bar{S}^{-1}(\bar{A}-L_p\bar{C})=-RP-PR-\bar{C}^{\top}\bar{C}\preceq -2P_1R \tag{16}$$

Let $R=\frac{1}{2}P_1^{-1}Q+\varrho I_{\bar{n}}$, where $\varrho>0$, then the inequality (12) can be obtained. □

Remark 4. *According to the observer error dynamics Equation (9), since $\bar{S}^{-1}$ has been determined by Lemma 1, the matrix L_p becomes the only parameter that can be used to configure the poles of dynamics (9). Although Lemma 2 provides the evidence that L_p exists, the structure of the UIO (3) introduces $\bar{S}^{-1}$, which makes it difficult to choose a suitable L_p. In practice, a suitable R can be selected according to (13), and then the matrix P can be solved from (14) by $vec(P)=(I_{\bar{n}}\otimes(R+\bar{S}^{-1}\bar{A})^{\top}+(R+\bar{S}^{-1}\bar{A})\otimes I_{\bar{n}})vec(\bar{C}^{\top}\bar{C})$, where $vec(M)$ represents the vector expression of a matrix M (See p. 30 in [39]).*

Before designing the FTC protocol, disassembling Equation (9) is required. First, taking $\bar{K}$ into (9) yields

$$\begin{aligned}\dot{\hat{\bar{x}}}_i=&\bar{S}^{-1}\left[(\bar{A}-L_p\bar{C})\hat{\bar{x}}_i-(\bar{A}-L_p\bar{C})\bar{S}^{-1}L_Dy_i+\bar{B}u_i+\bar{K}y_i+L_sv_{si}+L_D\bar{C}\dot{\bar{x}}_i\right]\\=&\bar{S}^{-1}\left[(\bar{A}-L_p\bar{C})\hat{\bar{x}}_i+L_py_i+\bar{B}u_i+L_sv_{si}+L_D\bar{C}\dot{\bar{x}}_i\right].\end{aligned} \tag{17}$$

Let $L_p \triangleq \left[L_{p1}^{\top},L_{p2}^{\top},L_{p3}^{\top}\right]$, where $L_{p1}\in\mathbb{R}^{n_x\times n_y}$, $L_{p1}\in\mathbb{R}^{n_{na}\times n_y}$, and $L_{p3}\in\mathbb{R}^{n_{ns}\times n_y}$. Substituding $\bar{S}$, L_p and L_D into (17), one can extract the differential equation of $\hat{x}_i$ as

$$\begin{aligned}\dot{\hat{x}}_i=&(A-L_{p1}C)\hat{x}_i+F_a\hat{f}_{ai}-L_{p1}F_s\hat{f}_{si}+L_{p1}Cx_i+L_{p1}F_sf_{si}+Bu_i\\=&A\hat{x}_i+F_a\hat{f}_{ai}-L_{p1}\bar{C}\tilde{\bar{x}}_i+Bu_i.\end{aligned} \tag{18}$$

For the sake of convenience, the FTC protocols discussed below are designed and discussed based on (18). It can be observed from (18) that $F_a\hat{f}_{ai}$ and $L_{p1}\bar{C}\tilde{\bar{x}}_i$ belong to disturbances. Therefore, we needs to cancel out these two terms in the design of FTC protocols if possible. Hereinafter, we will discuss the leaderless and leader–followers cases separately.

3.2. Leaderless FTC

Based on the estimation, an FTC protocol against actuator and sensor faults for leaderless MAS is proposed as

$$\begin{aligned}u_i=&-G\sum_{j=1}^{N}a_{ij}c_{ij}(\hat{x}_i-\hat{x}_j)-B^{+}F_a\hat{f}_{ai}\\\dot{c}_{ij}=&a_{ij}k_{ij}(\hat{x}_i-\hat{x}_j)^{\top}\Gamma(\hat{x}_i-\hat{x}_j),(i,j=1,\ldots,N),\end{aligned} \tag{19}$$

where $K=B^{\top}P_2$, $B^{+}=B^{\top}(BB^{\top})^{-1}$, $\Gamma\triangleq P_2BB^{\top}P_2$, and $P_2\in\mathbb{R}^{n_x\times n_x}$ is a positive definite matrix. Moreover, $c_{ij}(0)=c_{ji}(0)$ and $k_{ij}=k_{ij}$ are selected for all i and j.

The average estimated state is denoted by $\hat{x}^*\triangleq\frac{1}{N}\sum_{i=1}^{N}\hat{x}_i$. Let $e_i\triangleq\hat{x}_i-\hat{x}^*$ be the consensus error, the following equations can be obtained

$$\sum_{j=1}^{N}a_{ij}c_{ij}(\hat{x}_i-\hat{x}_j)=\sum_{j=1}^{N}a_{ij}c_{ij}(\hat{x}_i-\hat{x}^*+\hat{x}^*-\hat{x}_j)=\sum_{j=1}^{N}a_{ij}c_{ij}(\hat{e}_i-\hat{e}_j). \tag{20}$$

It can be obtained from (19) and $c_{ij}(0) = c_{ji}(0)$ that $c_{ij} = c_{ji}$ holds for $t \geq 0$, and $\sum_{j=1}^{N}\sum_{j=1}^{N} a_{ij}c_{ij}(\hat{x}_i - \hat{x}_j) = 0$. Furthermore, Assumption 4 gives $BB^{+}F_a = F_a$. Hence, the consensus error dynamics can be derived as

$$\dot{e}_i = Ae_i - L_{p1}\bar{C}(\tilde{\bar{x}}_i - \frac{1}{N}\sum_{j=1}^{N}\bar{x}_j) - BG\sum_{j=1}^{N} a_{ij}c_{ij}(\hat{e}_i - \hat{e}_j). \tag{21}$$

Imcorporating (10) and (21) yields the close-loop dynamics of the MAS

$$\begin{cases} \dot{\tilde{\bar{x}}}_i = \bar{S}^{-1}\left[(\bar{A} - L_p\bar{C})\tilde{\bar{x}}_i - \bar{F}\bar{f}_i + L_s v_{si}\right] \\ \dot{e}_i = Ae_i - L_{p1}\bar{C}(\tilde{\bar{x}}_i - \frac{1}{N}\sum_{j=1}^{N}\bar{x}_j) - BG\sum_{j=1}^{N} a_{ij}c_{ij}(e_i - e_j), (i,j = 1,\ldots,N). \end{cases} \tag{22}$$

Theorem 1. *The closed-loop dynamics (22) is stable and the consensus is achieved if there exist positive definite matrix P_1 and P_2 such that*

$$P_1\bar{S}^{-1}(\bar{A} - L_p\bar{C}) + (\bar{A} - L_p\bar{C})^{\top}\bar{S}^{-\top}P_1 + \frac{1}{\kappa}\bar{C}^{\top}L_{p1}^{\top}L_{p1}\bar{C} \prec 0, \tag{23a}$$

$$P_2A + A^{\top}P_2 - 2\alpha\lambda_i(\mathcal{L})P_2BB^{\top}P_2 + \kappa P_2P_2 \prec 0, \tag{23b}$$

hold for all $i = 1,\ldots,N$.

Proof. The stability analysis is conducted by estabilishing the following Lyapunov function

$$V = V_1 + V_2 + V_3, V_1 = \sum_{i=1}^{N}\tilde{\bar{x}}_i^{\top}P_1\tilde{\bar{x}}_i, V_2 = \sum_{i=1}^{N}e_i^{\top}P_2e_i, V_3 = \sum_{i=1}^{N}\sum_{j=1}^{N}\frac{(c_{ij} - \alpha)^2}{2k_{ij}}. \tag{24}$$

Taking the time derivative to V_1 renders

$$\begin{aligned} \dot{V}_1 &= \sum_{i=1}^{N}(\tilde{\bar{x}}_i^{\top}P_1\dot{\tilde{\bar{x}}}_i + \dot{\tilde{\bar{x}}}_i^{\top}P_1\tilde{\bar{x}}_i) \\ &= \sum_{i=1}^{N}\tilde{\bar{x}}_i^{\top}\left[P_1\bar{S}^{-1}(\bar{A} - L_p\bar{C}) + (\bar{A} - L_p\bar{C})^{\top}\bar{S}^{-\top}P\right]\tilde{\bar{x}}_i \\ &\quad - \sum_{i=1}^{N}2\tilde{\bar{x}}_i^{\top}P_1\bar{S}^{-1}\bar{F}\bar{f}_i + \sum_{i=1}^{N}2\tilde{\bar{x}}_i^{\top}P_1\bar{S}^{-1}L_sv_{si}. \end{aligned} \tag{25}$$

It follows from Assumption 2 that

$$-\sum_{i=1}^{N}\tilde{\bar{x}}_i^{\top}P\bar{S}^{-1}\bar{F}\bar{f}_i \leq \sum_{i=1}^{N}\|\bar{f}_i\|\|\tilde{\bar{x}}_i^{\top}P\bar{S}^{-1}\bar{F}\| \leq \sum_{i=1}^{N}(r_a + r_{ad} + r_s)\|s_i\|. \tag{26}$$

By recalling $(P_2\bar{S}^{-1}\bar{F})^{\top} = H\bar{C}$, it can be inferred that

$$\begin{aligned} \sum_{i=1}^{N}\tilde{\bar{x}}_i^{\top}P\bar{S}^{-1}L_sv_{si} &= -\sum_{i=1}^{N}(r_a + r_{ad} + r_s + \epsilon)\tilde{\bar{x}}_i^{\top}P\bar{S}^{-1}\bar{F}\text{sign}(H\bar{C}\tilde{\bar{x}}_i) \\ &= -\sum_{i=1}^{N}(r_a + r_{ad} + r_s + \epsilon)\|s_i\|. \end{aligned} \tag{27}$$

Therefore, incorporating (26) and (27) gives

$$-\sum_{i=1}^{N}\tilde{\bar{x}}_i^{\top}P\bar{S}^{-1}\bar{F}\bar{f}_i + \sum_{i=1}^{N}\tilde{\bar{x}}_i^{\top}P\bar{S}^{-1}L_sv_{si} \leq -\sum_{i=1}^{N}\epsilon\|s_i\|. \tag{28}$$

The time derivative of V_2 has

$$\dot{V}_2 = \sum_{i=1}^{N} e_i^\top (P_2 A + A^\top P_2) e_i - 2\sum_{i=1}^{N} e_i^\top P_2 L_{p1} \bar{C}(\tilde{\hat{x}}_i - \frac{1}{N}\sum_{j=1}^{N} \tilde{\hat{x}}_j) - 2\sum_{i=1}^{N} e_i^\top P_2 BG \sum_{j=1}^{N} a_{ij} c_{ij} (e_i - e_j) \tag{29}$$

Denote $\mathcal{M} \triangleq I_N - \frac{1}{N} 1_n^\top 1_n$, $e \triangleq \left[e_1^\top, \ldots, e_N^\top\right]^\top$, and $\tilde{\hat{x}} \triangleq \left[\tilde{\hat{x}}_1^\top, \ldots, \tilde{\hat{x}}_N^\top\right]^\top$. By applying Young's inequality, it can be deduced that

$$\begin{aligned} &-2\sum_{i=1}^{N} e_i^\top P_2 L_{p1} \bar{C}(\tilde{\hat{x}}_i - \frac{1}{N}\sum_{j=1}^{N} \tilde{\hat{x}}_j) \\ =&2e^\top \mathcal{M} \otimes P_2 L_{p1} \bar{C} \tilde{\hat{x}} \\ \leq&\kappa e^\top \mathcal{M}\mathcal{M}^\top \otimes P_2 P_2 e + \frac{1}{\kappa} \tilde{\hat{x}}^\top I_N \otimes \bar{C}^\top L_{p1}^\top L_{p1} \bar{C} \tilde{\hat{x}} \\ =&\kappa e^\top \mathcal{M}\mathcal{M} \otimes P_2 P_2 e + \frac{1}{\kappa} \sum_{i=1}^{N} \tilde{\hat{x}}_i^\top \bar{C}^\top L_{p1}^\top L_{p1} \bar{C} \tilde{\hat{x}}_i \end{aligned} \tag{30}$$

It worth noting that $\mathcal{M}$ is idempotent matrix, which indicates $\mathcal{M}\mathcal{M} = \mathcal{M}$. Further, one can derive that $\sum_{i=1}^{N} e_i = \sum_{i=1}^{N} (\hat{x}_i - \frac{1}{N}\sum_{j=1}^{N} \hat{x}_j) = 0$ and

$$e^\top \mathcal{M}\mathcal{M} \otimes P_2 P_2 e = e^\top \mathcal{M} \otimes P_2 P_2 e = \sum_{i=1}^{N} e_i^\top P_2 P_2 (e_i - \frac{1}{N}\sum_{j=1}^{N} e_j) = \sum_{i=1}^{N} e_i^\top P_2 P_2 e_i. \tag{31}$$

The time derivative of V_3 renders

$$\begin{aligned} \dot{V}_3 =& \sum_{i=1}^{N} \sum_{j=1, j\neq i}^{N} a_{ij} (c_{ij} - \alpha)(e_i - e_j)^\top \Gamma (e_i - e_j) \\ =&2\sum_{i=1}^{N} \sum_{j=1}^{N} a_{ij} (c_{ij} - \alpha) e_i^\top \Gamma (e_i - e_j). \end{aligned} \tag{32}$$

Because $\mathcal{G}$ is connected, there exists a unitary matrix $U = \left[\frac{1_{N\times 1}}{\sqrt{N}}, Y\right]$ such that $U^\top \mathcal{L} U = \Lambda = \mathrm{diag}(\lambda_1, \ldots, \lambda_N)$. Let $\xi \triangleq \left[\xi_1^\top, \ldots, \xi_N^\top\right]^\top = U \otimes I_{n_x} e$. Notice that $\mathcal{M} 1_{N\times 1} = 0$, hence

$$\xi_1 = \frac{1_{N\times 1}}{\sqrt{N}} \otimes P_2 e = \frac{\mathcal{M} 1_{N\times 1}}{\sqrt{N}} \otimes P_2 \hat{x} = 0. \tag{33}$$

Moreover, one has

$$\sum_{i=1}^{N} \sum_{j=1}^{N} a_{ij} e_i^\top \Gamma (e_i - e_j) = e^\top \mathcal{L} \otimes \Gamma e = \xi^\top \Lambda \otimes \Gamma \xi = \sum_{i=2}^{N} \lambda_i(\mathcal{L}) \xi_i^\top \Gamma \xi_i \tag{34}$$

By imcorporating (25)-(34), one can derived that

$$\begin{aligned} \dot{V} \leq& \sum_{i=1}^{N} \tilde{\hat{x}}_i^\top \left[P_1 \bar{S}^{-1}(\bar{A} - L_p \bar{C}) + (\bar{A} - L_p \bar{C})^\top \bar{S}^{-\top} P + \frac{1}{\kappa} \bar{C}^\top L_{p1}^\top L_{p1} \bar{C}\right] \tilde{\hat{x}}_i \\ &+ \sum_{i=2}^{N} \xi_i^\top (P_2 A + A^\top P_2 - 2\alpha \lambda_i(\mathcal{L}) P_2 B B^\top P_2 + \kappa P_2 P_2) \xi_i - \sum_{i=1}^{N} \epsilon \|s_i\| \end{aligned} \tag{35}$$

Therefore, one can derive $\dot{V} < 0$, which indicates that $\tilde{\hat{x}}_i$ and $e_i, (i = 1, \ldots, N)$ will reach convergence eventually, and further implies that $x_i - \frac{1}{N}\sum_{j=1}^{N} x_j$ is stable. Hence the proof is complete. □

3.3. Leader-Follower FTC

Consider a MAS consisting of N follower agents and one virtual leader. It is assumed that the communication topology among the followers is undirected and connected, and there is at least one follower has access to the leader's information. The dynamics of the N followers are given by (1), and the dynamics of the virtual leader agent are described as follows.

$$\dot{x}_0 = Ax_0. \tag{36}$$

The following adaptive FTC protocol based on estimation is proposed.

$$\begin{aligned} u_i =& -K^* \left[\sum_{j=1}^{N} a_{ij}c_{ij}(\hat{x}_i - \hat{x}_j) + b_i c_i (\hat{x}_i - x_0) \right] - B^+ F_a \hat{f}_{ai} \\ \dot{c}_{ij} =& a_{ij}k_{ij}(\hat{x}_i - \hat{x}_j)^\top \Gamma (\hat{x}_i - \hat{x}_j) \\ \dot{c}_i =& b_i k_i (\hat{x}_i - x_0)^\top \Gamma (\hat{x}_i - x_0). \end{aligned} \tag{37}$$

where $K^* = B^\top P_3$, $k_i > 0$, $k_{ij} > 0$, $\Gamma \triangleq P_3 B B^\top P_3$, and $P_3 \in \mathbb{R}^{n_x \times n_x}$ is a positive definite matrix. In addition, $c_{ij}(0) = c_{ji}(0)$ for all i and j.

Denote the tracking error by $\varsigma_i \triangleq \hat{x}_i - x_0$. Since $c_{ij} = c_{ji}$, it follows that $\sum_{j=1}^{N} a_{ij}c_{ij}(\hat{x}_i - \hat{x}_j) = \sum_{j=1}^{N} a_{ij}c_{ij}(\varsigma_i - \varsigma_j)$ and

$$\dot{\varsigma}_i = A\varsigma_i - L_{p1}\bar{C}\tilde{\bar{x}}_i - BR \left[\sum_{j=1}^{N} a_{ij}c_{ij}(\varsigma_i - \varsigma_j) + b_i c_i \varsigma_i \right]. \tag{38}$$

By combining (10) and (38), the overall close-loop dynamics is obtained

$$\begin{cases} \bar{S}\dot{\tilde{\bar{x}}}_i = (\bar{A} - L_p\bar{C})\tilde{\bar{x}}_i - \bar{F}\bar{f}_i + Fv_{si} \\ \dot{\varsigma}_i = A\varsigma_i - L_{p1}\bar{C}\tilde{\bar{x}}_i - BR \left[\sum_{j=1}^{N} a_{ij}c_{ij}(\varsigma_i - \varsigma_j) + b_i c_i \varsigma_i \right]. \end{cases} \tag{39}$$

Theorem 2. *The closed-loop dynamics (39) is stable and the tracking reaches convergence if there exist positive definite matrix P_1 and P_3 such that*

$$P_1\bar{S}^{-1}(\bar{A} - L_p\bar{C}) + (\bar{A} - L_p\bar{C})^\top \bar{S}^{-\top} P_1 + \frac{1}{\kappa}\bar{C}^\top L_{p1}^\top L_{p1}\bar{C} \prec 0 \tag{40a}$$

$$P_3 A + A^\top P_3 - 2\beta\lambda_i(\mathcal{H}) P_3 B B^\top P_3 + \kappa P_3 P_3 \prec 0 \tag{40b}$$

hold for all $i = 1, \ldots, N$.

Proof. Consider the following Lyapunov function

$$\begin{aligned} &V = V_1 + V_2 + V_3 + V_4 \\ &V_1 = \sum_{i=1}^{N} \tilde{\bar{x}}_i^\top P_1 \tilde{\bar{x}}_i, V_2 = \sum_{i=1}^{N} \varsigma_i^\top P_3 \varsigma_i, V_3 = \sum_{i=1}^{N} \sum_{j=1, j\neq i}^{N} \frac{(c_{ij} - \beta)^2}{2k_{ij}}, V_4 = \sum_{i=1}^{N} \sum_{j=1}^{N} \frac{(c_i - \beta)^2}{2k_{ij}}. \end{aligned} \tag{41}$$

Taking the time derivative to V_2 gives

$$\begin{aligned} \dot{V}_2 = &\sum_{i=1}^{N} \varsigma_i^\top (P_3 A + A^\top P_3)\varsigma_i - 2\sum_{i=1}^{N} \varsigma_i^\top P_3 L_{p1}\bar{C}\tilde{\bar{x}}_i \\ &- 2\sum_{i=1}^{N} \varsigma_i^\top P_3 BG \sum_{j=1}^{N} a_{ij}c_{ij}(\varsigma_i - \varsigma_j) - 2\sum_{i=1}^{N} \varsigma_i^\top P_3 BG \sum_{j=1}^{N} d_i c_i \varsigma_i. \end{aligned} \tag{42}$$

By applying Young's inequality, one can derive

$$-2\sum_{i=1}^{N}\varsigma_i^\top P_3 L_{p1}\bar{C}\tilde{\bar{x}}_i \le \sum_{i=1}^{N}\kappa\varsigma_i^\top P_3 P_3\varsigma_i + \sum_{i=1}^{N}\frac{1}{\kappa}\tilde{\bar{x}}_i^\top \bar{C}^\top L_{p1}^\top L_{p1}\bar{C}\tilde{\bar{x}}_i. \tag{43}$$

Similar to the leaderless case, the time derivative of V_3 and V_4 gives

$$\begin{aligned}\dot{V}_3 =& \sum_{i=1}^{N}\sum_{j=1,j\neq i}^{N} a_{ij}(c_{ij}-\beta)(\varsigma_i-\varsigma_j)^\top\Gamma(\varsigma_i-\varsigma_j)\\ =&2\sum_{i=1}^{N}\sum_{j=1}^{N} a_{ij}(c_{ij}-\beta)\varsigma_i^\top\Gamma(\varsigma_i-\varsigma_j),\end{aligned} \tag{44}$$

and

$$\dot{V}_4 = \sum_{i=1}^{N}\sum_{j=1}^{N} b_i(c_i-\beta)\varsigma_i^\top\Gamma\varsigma_i = 2\sum_{i=1}^{N} b_i(c_i-\beta)\varsigma_i^\top\Gamma\varsigma_i. \tag{45}$$

There exists a unitary matrix U such that $\Omega = U^\top\mathcal{H}U = \mathrm{diag}(\lambda_1(\mathcal{H}),\ldots,\lambda_N(\mathcal{H}))$ for $\mathcal{H} = \mathcal{L}+\mathcal{B}$. Let $\varsigma \triangleq \left[\varsigma_1^\top,\ldots,\varsigma_N^\top\right]^\top$, and $\zeta \triangleq \left[\zeta_1^\top,\ldots,\zeta_N^\top\right]^\top = U\otimes I_{n_x}\varsigma$. Hence, one can derive that

$$\begin{aligned}&\varsigma^\top\Big[I_N\otimes(P_3A+A^\top P_3+\kappa P_3P_3)-2\beta\mathcal{H}\otimes P_3BB^\top P_3\Big]\varsigma\\ =&\zeta^\top\Big[I_N\otimes(P_3A+A^\top P_3+\kappa P_3P_3)-2\beta\Omega\otimes P_3BB^\top P_3\Big]\zeta\\ =&\sum_{i=1}^{N}\zeta_i^\top\Big[P_3A+A^\top P_3+\kappa P_3P_3-2\beta\lambda_i(\mathcal{H})P_3BB^\top P_2\Big]\zeta_i\end{aligned} \tag{46}$$

Imcorporating (41)–(46) and (25) yields

$$\begin{aligned}\dot{V} =&\dot{V}_1+\dot{V}_2+\dot{V}_3+\dot{V}_4\\ \le&\sum_{i=1}^{N}\tilde{\bar{x}}_i^\top\Big[P_1\bar{S}^{-1}(\bar{A}-L_p\bar{C})+(\bar{A}-L_p\bar{C})^\top\bar{S}^{-\top}P+\frac{1}{\kappa}\bar{C}^\top L_{p1}^\top L_{p1}\bar{C}\Big]\tilde{\bar{x}}_i\\ &+\sum_{i=1}^{N}\zeta_i^\top\Big[P_3A+A^\top P_3+\kappa P_3P_3-2\beta\lambda_i(\mathcal{H})P_3BB^\top P_2\Big]\zeta_i-\sum_{i=1}^{N}\epsilon\|s_i\|.\end{aligned} \tag{47}$$

In the light of Theorem 2, one has $\dot{V}<0$, which means that $\tilde{\bar{x}}_i$ and $\varsigma_i,(i=1,\ldots,N)$ is stable, and further implies that x_i-x_0 is stable. This ends the proof. □

Remark 5. *It should be noted that since $\bar{C}$ is not column full rank matrix. This means $\bar{C}^+\bar{C}\neq I_{n_y}$, and H cannot be calculated with $H=(P\bar{S}^{-1}\bar{F})^\top\bar{C}^+$. However, we can use the Schur complement to obtain an approximate solution. The H matrix subject to the condition $(P\bar{S}^{-1}\bar{F})^\top = H\bar{C}$, which is equivalent to*

$$Trace\Big[(\bar{F}^\top\bar{S}^{-\top}P-H\bar{C})^\top(\bar{F}^\top\bar{S}^{-\top}P-H\bar{C})\Big]=0. \tag{48}$$

The above equation can be approximated by

$$(\bar{F}^\top\bar{S}^{-\top}P-H\bar{C})^\top(\bar{F}^\top\bar{S}^{-\top}P-H\bar{C})\prec\varepsilon I, \tag{49}$$

where $\varepsilon>0$ is small constant.

Furthermore, by applying Schur complement, the above LMI can be transformed into

$$\begin{bmatrix}-\varepsilon I_{\bar{n}} & (\bar{F}^\top\bar{S}^{-\top}P-H\bar{C})^\top\\ * & -I_{p+q}\end{bmatrix}\prec 0, \tag{50}$$

of which the solution is much easier to find.

Proposition 1. *Replacing the existing undirected graph with a connected directed graph will not affect the results in the subsequent discussion of Lyapunov functions, and the convergence is still guaranteed. It is worth noting that $L + L^\top$ can be deemed as the Laplacian matrix of a new undirected graph. Based on the fact that the feedback gain matrices are determined by $K = B^\top P_2$ and $K^* = B^\top P_3$ in the FTC scheme, one can derive from the Lyapunov function analysis that the same conclusions can be drawn if the graph is directed and connected.*

Remark 6. *The convergence of observation error $\tilde{\hat{x}}_i$ implies the estimations of the system state, actuator fault, and sensor fault are simultaneously achieved, which can be calculated by $\hat{x}_i = \left[I_{n_x}, 0_{n_x \times (n_a+n_s)}\right]\hat{\hat{x}}_i$, $\hat{f}_{ai} = [0_{n_a \times n_x}, I_{n_a}, 0_{n_a \times n_s}]\hat{\hat{x}}_i$ and $\hat{f}_{si} = [0_{n_s \times n_x}, 0_{n_s \times n_a}, I_{n_s}]\hat{\hat{x}}_i$, respectively.*

Remark 7. *Although the FTC protocols (19) and (37) are designed based on the dynamics of $\hat{x}_i$, they serve as actual control laws for the MASs. This is because when $\tilde{\hat{x}}_i = 0$, $\hat{x}_i = x^*$ implies that $x_i = x^*$. The choice to use the dynamics of $\hat{x}_i$ in the formulas is purely for the convenience of mathematical derivation.*

Remark 8. *The FTC scheme consists of a local observer and a distributed controller for leaderless/leader–follower case, where the distributed FTC protocols (19) and (37) utilize estimations gathered from the observer (3). The magnitude of the consensus error depends on two factors: the estimation error of the observer and the consensus error of the distributed controller. From the analysis result of Theorems 1 and 2, one can see that both errors are temporary and will eventually converge to zero. Nevertheless, it is worth pointing out that the convergence speed of the distributed controller will decrease as the number of agents increases, whereas the tracking speed of the local observer is only related to the system's and observer's parameters. Hence, the parameter selections of the observer can be decoupled from the FTC protocols where one can obtain a satisfying FTC performance by choosing a suitable L_p such that the poles of (10) are as far away from the right half plane as possible and as close to the real axis as possible for a desired dynamics characteristics.*

4. Simulation Results

In this section, simulations of leaderless and leader–follower MAS are provided to demonstrate the effectiveness of the proposed FTC protocols.

The parameter matrices for the agents' dynamics are as given as follows.

$$A = \begin{bmatrix} -3 & -1 & \\ & -3 & \\ 2 & 1 & -2 \end{bmatrix}, B = \begin{bmatrix} 0 \\ 1 \\ 2 \end{bmatrix}, F_a = B, F_s = \begin{bmatrix} 0 \\ 1 \\ 2 \end{bmatrix}, C = \begin{bmatrix} 1 & & \\ & 2 & \\ & & 1 \end{bmatrix}$$

The parameters are set as $\kappa = 1$, $\alpha = \frac{1}{\lambda_2(\mathcal{L})}$, $\beta = \frac{1}{\lambda_{\min}(\mathcal{H})}$, and the following matrices are selected for the observer and FTC protocols.

$$\begin{aligned} P_1 &= \begin{bmatrix} 2.75 \times 10^5 & -2360.9 & 7444.1 & -3.6202 & 10439 \\ -2360.9 & 1812.1 & 260.99 & -0.026 & 1669.6 \\ 7444.1 & 260.99 & 669.54 & -0.025 & 1348.8 \\ -3.62 & -0.026 & -0.025 & 0.003 & -0.06 \\ 10439 & 1669.6 & 1348.8 & -0.0634 & 3532.3 \end{bmatrix}, H = \begin{bmatrix} -3.62 & -0.013 & -0.025 \\ 83.51 & 6.68 & 10.79 \\ 0.59 & 165.27 & -18.45 \end{bmatrix} \\ L_p &= \begin{bmatrix} 33.86 & -1.29 & 1.92 \\ -0.37 & 374.2 & -40.44 \\ 3.02 & 807 & -54.15 \\ -117.56 & 52171 & -6071.7 \\ 63.9 & 6612.8 & 1363 \end{bmatrix}, P_2 = P_3 = \begin{bmatrix} 0.44 & -0.09 & 0.12 \\ -0.09 & 0.35 & -0.034 \\ 0.12 & -0.034 & 0.33 \end{bmatrix}. \end{aligned} \tag{51}$$

4.1. Leaderless FTC

In the leaderless case, suppose that the MAS consists of four agents among which the connections are as shown in Figure 1.

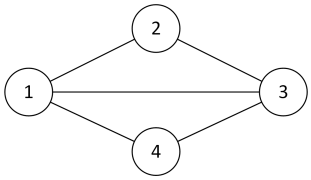

Figure 1. Communication topology of the leaderless MAS.

The following actuator and sensor faults are injected into the leaderless MAS in the simulation. The rest of the agents remains fault-free in the simulation.

$$\begin{aligned} f_{a1} &= 12\sin(0.5t + 0.5\pi), \quad (t \geq 10\text{ s}) \\ f_{s1} &= 10\sin(0.8t), \quad (t \geq 5\text{ s}) \\ f_{a3} &= 10\sin(0.5t + 0.5\pi), \quad (t \geq 5\text{ s}) \\ f_{s3} &= 12\sin(0.8t), \quad (t \geq 10\text{ s}). \end{aligned}$$

The simulation results are presented in Figure 2. As shown in Figure 2a, the MAS states converge to a stable range within $t \leq 3$ s, and then experience disturbances at $t \geq 5$ s and $t \geq 10$ s due to faults injection. However, the tracking error $\tilde{x}_{1\sim4}$ remains upper-bounded by $\|\tilde{x}_{1\sim4}\| \leq 0.5$, which is acceptable considering the magnitude of the faults. From Figure 2a,b, the dashed and solid lines almost overlap with each other, indicating that the observer accurately estimated the states and faults of the MAS quickly. Moreover, as shown in Figure 2c, even if multiple faults occur in the MAS, the overall convergence performance is satisfactory, and the consensus error is bouned by $\|e_{1\sim4}\| \leq 0.5$, verifying the effectiveness and demonstrating the performance of the proposed observer (3) and distributed FTC protocol (19) for leaderless MAS against concurrent actuator and sensor faults.

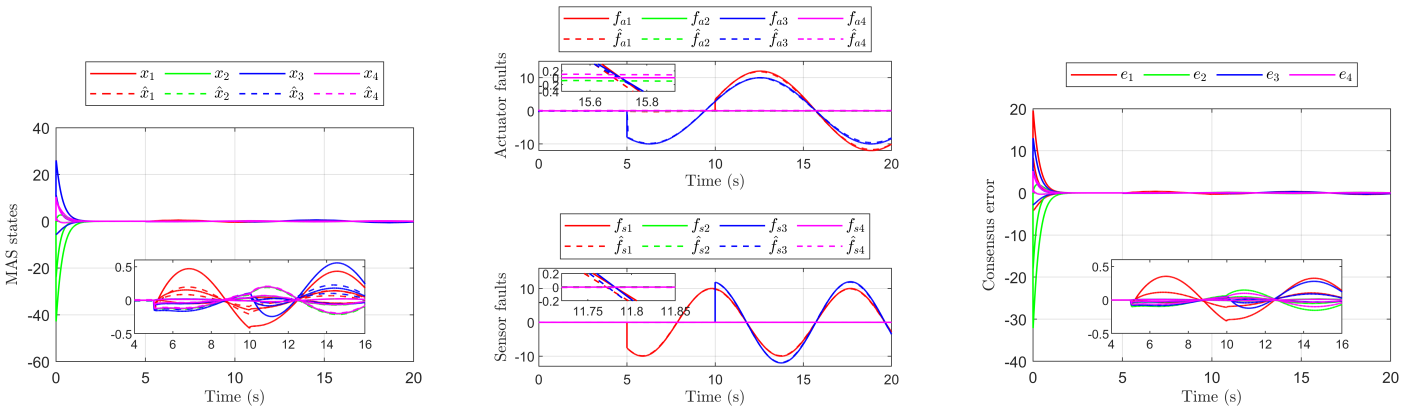

(**a**) (**b**) (**c**)

Figure 2. Simulation results of the leaderless case. (**a**) MAS states and their estimations. (**b**) Faults and their estimations. (**c**) MAS consensus error.

4.2. Leader-Follower FTC

In the leader–follower case, suppose that the MAS consists of four followers and one virtual leader, among which the connections are as shown in Figure 3.

The following actuator and sensor faults are injected into the leader–follower MAS. The rest of the agents remains fault-free in the simulation.

$$\begin{aligned} f_{a1} &= 5\sin(t + 0.5\pi), \quad t \geq 10\text{ s} \\ f_{s1} &= 6\sin(0.8t), \quad t \geq 5\text{ s} \\ f_{a3} &= 6\sin(t + 0.5\pi), \quad t \geq 6\text{ s} \\ f_{s3} &= 5\sin(0.8t), \quad t \geq 10\text{ s}. \end{aligned}$$

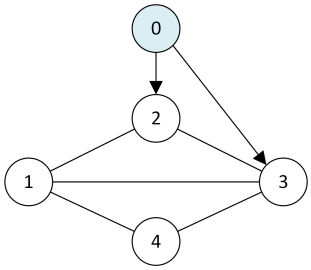

Figure 3. Communication topology of the leader–follower MAS.

The simulation results are shown in Figure 4. It can be observed from the Figure 4a that the state of the MAS converges to a stable for $t \leq 3$ s. As the amplitudes of the injected faults are relatively smaller than that under the leaderless scenario, there is no significant change in the overall stability of the MAS states $x_{1\sim4}$ at the time of injecting faults into the system, i.e., $t \geq 5$ s and $t \geq 10$ s. According to the results plotted in Figure 4c, even when multiple faults occur in the MAS, the tracking error is contained within a small region $\|\xi_{1\sim4}\| \leq 0.5$. This suggests that the FTC protocol (37) can effectively resist the interference caused by actuator and sensor faults.

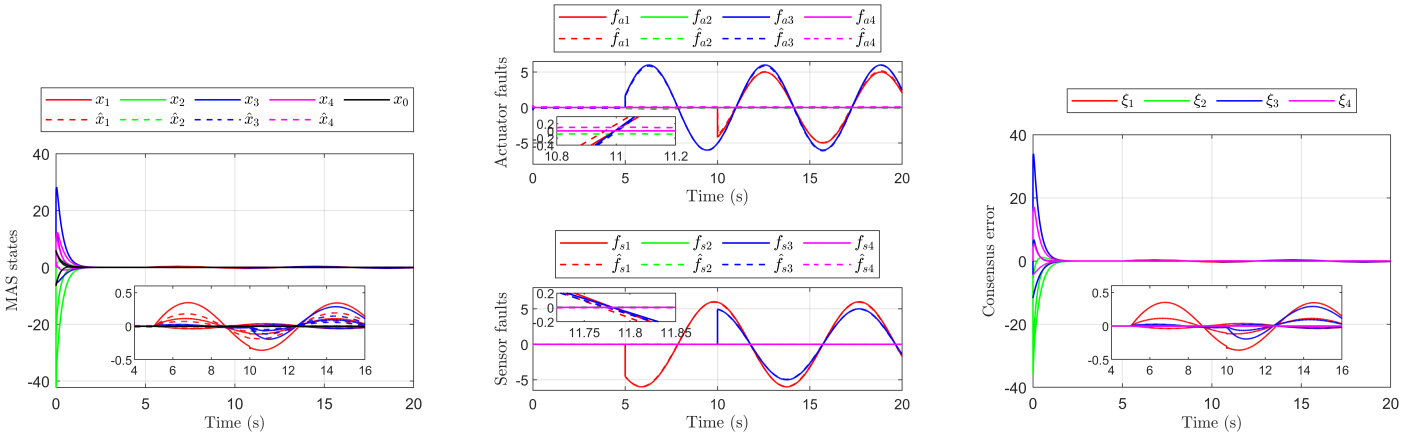

(**a**) (**b**) (**c**)

Figure 4. Simulation results of the leader–follower case. (**a**) MAS states and their estimations. (**b**) Faults and their estimations. (**c**) MAS tracking error.

According to the simulation results, under both leaderless and leader–follower structures, the proposed FTC scheme can effectively maintain the stability of the MAS in the presence of actuator and sensor faults. In both cases, the estimation errors of the MAS states satisfy $\|\tilde{x}_{1\sim4}\| \leq 0.5$ in the steady state, the estimation errors of the faults satisfy $\|f_{a1\sim4}\| \leq 0.2$ and $\|f_{s1\sim4}\| \leq 0.2$, the control errors satisfy $\|e_{1\sim4}\| \leq 0.5$ and $\|\xi_{1\sim4}\| \leq 0.5$. Moreover, the time for the MAS to reach the steady state satisfies $t \leq 3$ s. In conclusion, the proposed observer-based FTC scheme shows satisfactory performance under the concurrent faults situations.

5. Conclusions

In summary, this paper proposes an effective approach to deal with the abnormal operation or even fault of leaderless/leader–follower MASs caused by actuator and sensor faults. Firstly, an extended state is constructed by integrating faults as components, and the MAS dynamics are transformed into a descriptor system form. Then, a sliding mode-based UIO is designed for the transformed system. Based on the estimation obtained from the observer, adaptive FTC algorithms are developed for leaderless/leader–follower MAS separately, in which the control gains are updated with the distributed tracking error. Finally, numerical simulations show that the proposed method can guarantee the stability of the MAS against actuator and sensor faults.

This paper is a useful attempt in the research direction of distributed FTC against sensor fault, which provides theoretical support for improving the MAS's reliability and has certain theoretical value and engineering application prospects. However, the method proposed in this paper also has some limitations. For example, it is difficult to handle the case where MAS has nonlinear dynamics, and ideal communication conditions such as undirected graph and unlimited communication capability are assumed in the discussion.

Future research directions can be extended to switching topology with transmission delays; machine learning-based nonlinearity cancellation; MAS with heterogeneous dynamics and adaptive technique for local observers, etc. In summary, concerning various scenarios and applications, the theory and methods of FTC for MASs against actuator and sensor faults have broad research prospects.

Author Contributions: Conceptualization, Y.C. and Z.Y. (Ziquan Yu); methodology, validation, writing—original draft preparation, Z.Y. (Zhengyu Ye); writing—review and editing, Z.Y. (Ziquan Yu), Z.Y. (Zhengyu Ye); supervision, B.J.; project administration, Y.C. and Z.Y. (Ziquan Yu); funding acquisition, B.J. All authors have read and agreed to the published version of the manuscript.

Funding: This research was funded by National Natural Science Foundation of China: 62020106003, and Natural Science Foundation of Jiangsu Province of China: BK20222012.

Data Availability Statement: Not applicable.

Conflicts of Interest: The authors declare no conflict of interest.

References

1. Yu, D.; Chen, C.; Ren, C.; Sui, S. Swarm control for self-organized system with fixed and switching topology. *IEEE Trans. Cybern.* **2020**, *50*, 4481–4494. [CrossRef] [PubMed]
2. Liang, X.; Qu, X.; Wang, N.; Li, Y.; Zhang, R. Swarm control with collision avoidance for multiple underactuated surface vehicles. *Ocean Eng.* **2019**, *191*, 106516. [CrossRef]
3. Yu, Z.; Liu, Z.; Zhang, Y.; Qu, Y.; Su, C. Distributed finite-time fault-tolerant containment control for multiple unmanned aerial vehicles. *IEEE Trans. Neural Netw. Learn. Syst.* **2020**, *31*, 2077–2091. [CrossRef] [PubMed]
4. Yu, Z.; Zhang, Y.; Jiang, B.; Su, C.; Fu, J.; Jin, Y.; Chai, T. Fractional-order adaptive fault-tolerant synchronization tracking control of networked fixed-wing uavs against actuator-sensor faults via intelligent learning mechanism. *IEEE Trans. Neural Netw. Learn. Syst.* **2021**, *32*, 5539–5553. [CrossRef]
5. Yu, Z.; Zhang, Y.; Jiang, B.; Su, C.; Fu, J.; Jin, Y.; Chai, T. Decentralized fractional-order backstepping fault-tolerant control of multi-uavs against actuator faults and wind effects. *Aerosp. Sci. Technol.* **2020**, *104*, 105939. [CrossRef]
6. Ding, D.; Han, Q.; Wang, Z.; Ge, X. A survey on model-based distributed control and filtering for industrial cyber-physical systems. *IEEE Trans. Ind. Inform.* **2019**, *15*, 2483–2499. [CrossRef]
7. Dohmann, P.; Hirche, S. Distributed control for cooperative manipulation with event-triggered communication. *IEEE Trans. Robot.* **2020**, *36*, 1038–1052. [CrossRef]
8. Tang, J.; Chen, X.; Zhu, X.; Zhu, F. Dynamic reallocation model of multiple unmanned aerial vehicle tasks in emergent adjustment scenarios. *IEEE Trans. Aerosp. Electron. Syst.* **2023**, *59*, 1139–1155. [CrossRef]
9. Wang, J.; Liu, M.; Sun, J.; Gui, G.; Gacanin, H.; Sari, H.; Adachi, F. Multiple unmanned-aerial-vehicles deployment and user pairing for nonorthogonal multiple access schemes. *IEEE Internet Things J.* **2021**, *8*, 1883–1895. [CrossRef]
10. Yao, W.; Qi, N.; Wan, N.; Liu, Y. An iterative strategy for task assignment and path planning of distributed multiple unmanned aerial vehicles. *Aerosp. Sci. Technol.* **2019**, *86*, 455–464. [CrossRef]
11. Kamel, M.; Yu, X.; Zhang, Y. Formation control and coordination of multiple unmanned ground vehicles in normal and faulty situations: A review. *Annu. Rev. Control* **2020**, *49*, 128–144. [CrossRef]
12. Jose, M.; Gonzalez-R, P.; Andrade-Pineda, J.; Canca, D.; Calle, M. A multi-agent approach to the truck multi-drone routing problem. *Expert Syst. Appl.* **2022**, *195*, 116604.
13. Gu, R.; Sun, X.; Pu, D. Adaptive fault-tolerant control for second-order multiagent systems with unknown control directions via a self-tuning distributed observer. *Electronics* **2022**, *11*, 3939. [CrossRef]
14. Ahmad, A.; Corchado, J.; O'neill, V.; Soh, B. Improving fault tolerance and reliability of heterogeneous multi-agent iot systems using intelligence transfer. *Electronics* **2022**, *11*, 2724.
15. Zhang, P.; Zhang, J.; Yang, J.; Gao, S. Resilient event-triggered adaptive cooperative fault-tolerant tracking control for multiagent systems under hybrid actuator faults and communication constraints. *IEEE Trans. Aerosp. Electron. Syst.* **2023**, *59*, 3021–3037. [CrossRef]
16. Huang, J.; Wang, W.; Wen, C.; Zhou, J.; Li, G. Distributed adaptive leader–follower and leaderless consensus control of a class of strict-feedback nonlinear systems: A unified approach. *Automatica* **2020**, *118*, 109021. [CrossRef]

17. Chen, C.; Lewis, F.L.; Li, X. Event-triggered coordination of multi-agent systems via a Lyapunov-based approach for leaderless consensus. *Automatica* **2022**, *136*, 109936. [CrossRef]
18. Zhang, J.; Feng, T. From undirected graphs to directed graphs: A new technique makes it possible for multi-agent systems. *J. Control Decis.* **2022**, *9*, 286–288.
19. Wang, L.; Zou, M.; Guo, W.; Alsubaie, H.; Alotaibi, A.; Taie, R.; Jahanshahi, H. Adaptive discontinuous control for fixed-time consensus of nonlinear multi-agent systems. *Electronics* **2022**, *11*, 3545. [CrossRef]
20. Wang, C.; Wang, J.; Wu, P.; Gao, J. Consensus problem and formation control for heterogeneous multi-agent systems with switching topologies. *Electronics* **2022**, *11*, 2598. [CrossRef]
21. Wei, Q.; Wang, X.; Zhong, X.; Wu, N. Consensus control of leader-following multi-agent systems in directed topology with heterogeneous disturbances. *IEEE/CAA J. Autom. Sin.* **2021**, *8*, 423–431. [CrossRef]
22. Abbaspour, A.; Mokhtari, S.; Sargolzaei, A.; Yen, K. A survey on active fault-tolerant control systems. *Electronics* **2020**, *9*, 1513. [CrossRef]
23. Wang, X.; Zhou, Y.; Huang, T.; Chakrabarti, P. Event-triggered adaptive fault-tolerant control for a class of nonlinear multiagent systems with sensor and actuator faults. *IEEE Trans. Circuits Syst. I Regul. Pap.* **2022**, *69*, 4203–4214. [CrossRef]
24. Guo, X.; Liu, P.; Wang, J.; Ahn, C. Event-triggered adaptive fault-tolerant pinning control for cluster consensus of heterogeneous nonlinear multi-agent systems under aperiodic dos attacks. *IEEE Trans. Netw. Sci. Eng.* **2021**, *8*, 1941–1956. [CrossRef]
25. Li, K.; Li, Y. Fuzzy adaptive optimal consensus fault-tolerant control for stochastic nonlinear multiagent systems. *IEEE Trans. Fuzzy Syst.* **2022**, *30*, 2870–2885. [CrossRef]
26. Ju, Y.; Tian, X.; Wei, G. Fault tolerant consensus control of multi-agent systems under dynamic event-triggered mechanisms. *ISA Trans.* **2022**, *127*, 178–187. [CrossRef] [PubMed]
27. Cheng, F.; Liang, H.; Wang, H.; Zong, G.; Xu, N. Adaptive neural self-triggered bipartite fault-tolerant control for nonlinear mass with dead-zone constraints. *IEEE Trans. Autom. Sci. Eng.* **2023**, *20*, 1663–1674. [CrossRef]
28. Liu, C.; Jiang, B.; Zhang, K.; Patton, R. Distributed fault-tolerant consensus tracking control of multi-agent systems under fixed and switching topologies. *IEEE Trans. Circuits Syst. I Regul. Pap.* **2021**, *68*, 1646–1658. [CrossRef]
29. Chen, S.; Daniel, W.; Li, L.; Liu, M. Fault-tolerant consensus of multi-agent system with distributed adaptive protocol. *IEEE Trans. Cybern.* **2015**, *45*, 2142–2155. [CrossRef]
30. Liu, F.; Hua, Y.; Dong, X.; Li, Q.; Ren, Z. Adaptive fault-tolerant time-varying formation tracking for multi-agent systems under actuator fault and input saturation. *ISA Trans.* **2020**, *104*, 145–153. [CrossRef]
31. Ye, D.; Chen, M.; Li, K. Observer-based distributed adaptive fault-tolerant containment control of multi-agent systems with general linear dynamics. *ISA Trans.* **2017**, *71*, 32–39. [CrossRef] [PubMed]
32. Liu, C.; Jiang, B.; Patton, R.; Zhang, K. Decentralized output sliding-mode fault-tolerant control for heterogeneous multiagent systems. *IEEE Trans. Cybern.* **2020**, *50*, 4934–4945. [CrossRef]
33. Deng, C.; Wen, C. Distributed resilient observer-based fault-tolerant control for heterogeneous multiagent systems under actuator faults and dos attacks. *IEEE Trans. Control Netw. Syst.* **2020**, *7*, 1308–1318. [CrossRef]
34. Zhang, K.; Jiang, B.; Yan, X.; Xia, J. Distributed fault diagnosis of multi-agent systems with time-varying sensor faults. *ICIC Exp. Lett.* **2020**, *14*, 129–135.
35. Sun, Y.; Xia, Y.; Zhang, J.; Ding, D. Adaptive fault-tolerant output regulation of linear multi-agent systems with sensor faults. *IEEE Access* **2020**, *8*, 159440–159448. [CrossRef]
36. Gong, J.; Jiang, B.; Shen, Q. Distributed-observer-based fault tolerant control design for nonlinear multi-agent systems. *Int. J. Control. Autom. Syst.* **2019**, *17*, 3149–3157. [CrossRef]
37. Choi, K.; Kim, Y.; Kim, S.; Kim, K. Current and position sensor fault diagnosis algorithm for pmsm drives based on robust state observer. *IEEE Trans. Ind. Electron.* **2021**, *68*, 5227–5236. [CrossRef]
38. Gao, L.; Li, D.; Yao, L.; Gao, Y. Sensor drift fault diagnosis for chiller system using deep recurrent canonical correlation analysis and k-nearest neighbor classifier. *ISA Trans.* **2022**, *122*, 232–246. [CrossRef]
39. Petersen, K.B.; Petersen, M.S. *The Matrix Cookbook*; Technical University of Denmark: Lyngby, Denmark, 2012.